Fatigue testing of glass/epoxy joints in timber up to the endurance limit.

P A Claisse, T J Davis and B Masse

Civil Engineering Group, Coventry University, Priory Street, Coventry, CV1 5FB

Phone: 024 7688 8881, Fax 024 7688 8296 Email: P.Claisse@coventry.ac.uk

Abstract

Concern about fatigue is one of the factors limiting use of glass/epoxy jointing systems for timber in construction. In this paper a series of high-cycle fatigue tests are reported which indicate that the performance is as good, if not superior to, conventional jointing systems. The performance of the joints was found to produce a straight line on a logarithmic S-N plot and thus be readily predictable for design purposes.

Keywords

Timber, glass fibre, epoxy, fatigue, timber joints

Introduction

Bonded glass fibre represents an attractive option for jointing and reinforcing timber in many circumstances. The glass is thoroughly wetted with the liquid resin and sets to give a finish which is strong, highly resistant to moisture and can have a good appearance because it is transparent and reveals the wood beneath it. Extensive use in small boat construction has exploited these properties. However Benham et al., (1) state "It has been, estimated that at least 75% of all machine and structural failures have been caused by some form of fatigue" and therefore data is required on the fatigue properties of the system before it can be used in construction. The aim of this paper is to contribute to that requirement for data on fatigue.

Literature Review

Fatigue tests are characterised by the R ratio which is defined as: $R = \frac{\sigma_{min}}{\sigma_{max}}$

where σ_{min} and σ_{max} are the minimum and maximum stresses applied during the cyclic loading. Ansell (2) presented data (figure 1) which summarises the properties of plain timber in fatigue. This shows that the number of cycles to failure depends on the stress (as a proportion of the maximum stress at failure in a static test) and the R ratio.

Relatively few authors have published data on wood/glass/epoxy composites in fatigue. Hacker and Ansell (3) have investigated property changes and fatigue damage accumulation of wood-epoxy laminates under constant amplitude fatigue tests in tension-tension (R = 0.1), compression-compression (R = 10) and reverse loading (R = -1). They found that the reverse loading is the most severe mode of cyclic loading. The wood appeared to be more tolerant in compression-compression than in tension-tension. Maximum and minimum fatigue strains were monitored during the fatigue tests. In tension-tension (R = 0.1), the strains remained constant through the test, but they increase significantly close to failure. The sudden increases of strains were found to correspond to the initiation and growth of fatigue cracks along the wood grain, as each crack initiation causes a small step in strain.

Spera et al. (4) investigated laminated Douglas fir/epoxy as materials for wind turbine blades. They characterised the fatigue properties of Douglas fir/epoxy joints. They tested scarf and butt joints in tension-tension at R = 0.1 with different grades and joint sizes. It appeared that the veneer grades do not govern the joint fatigue resistance: For the butt joints, the grade A veneer outperformed the grade A+ veneer, which is a higher quality grade. A further observed effect was that the increased surface area of the scarf joints did not translate into an increase in strength and fatigue resistance. This could be due the fact that larger bonded areas contain more voids and therefore the bond was significantly degraded.

Sutherland (5) presented a report containing a large research program about the applications of glass fibres in a resin matrix to build wind turbine blades that was undertaken in the early 1990s in United States. This program aimed at the development of a glass fibre composite database for wind turbine applications. The DOE/MSU database for E-glass composites contains over 4500 data points for 130 material systems tested. The high frequency database provides a significant data set for unidirectional composites to 10^8 cycles. The database explores material parameters such as reinforcement fabric architecture, fibre content, matrix materials and loading parameters (R values). The results gave good agreement with those in this paper as noted in the discussion .

Fatigue tests were carried out by Bainbridge et al. (6) on bonded-in rods in glued laminated timber, using three different types of adhesives: Epoxy, polyurethane and phenol resorcinol formaldehyde. Mild and high strength steel threaded rods were axially loaded in tension parallel to the grain of the timber at a frequency of 1Hz. S-N curves were presented for an R ratio of 0.1. The authors investigated the relationship between experimental results and the design code basis, trying to establish fatigue coefficients by comparison of the results with existing data. Fatigue coefficients were not evaluated because of the limited number of load cycles.

Experimental Method

A screw driven testing machine was selected to carry out the fatigue tests. This machine is equipped with a 100 kN load cell that works in tension and compression. The machine was used with a PC and a data acquisition system which received data from Linear Voltage Displacement Transducers (LVDTs) and resistance strain gauges (7). The frequency of loading in the fatigue tests was intended to simulate wind loading for which 3 second gusts were used in CP3: Ch 5: Pt 2 (8). The more recent standard (BS6399-2) is based on an hourly mean value which is converted into a gust speed by the application of a gust peak factor but does not specify a time which could be used to determine a cyclic loading frequency.

A 3 second period corresponds to fairly fast loading and unloading rates, particularly if the maximum load is as high as 30 kN. The test equipment could load and unload a joint to that range of loading rate, but the speed of the crosshead was such that it could not stop at 0 kN precisely. The crosshead would tend to unload further and apply some compression to the sample. In order to make sure the sample was never subjected to compressive stress, it was decided to limit the minimum stress to 10% of the maximum stress, to have a loading condition with an R ratio of 0.1.

Sample fabrication.

Timber samples were European Spruce graded C16 to C24 to BS5268 Part 2 (9). The samples had nominal cross section 100mm by 50mm and were cut from four planks which are designated A, B, C and D in the data tables. Unidirectional glass fibre woven roving (SP Systems product code UT-E500 (10)) was selected for the joints. In this cloth almost all of the fibres are uni-directional with just a very light weave across them to hold them in place during fabrication. The epoxy was a clear coating/laminating

resin (SP Systems product code Spabond 120 (10)) which was used with slow hardener at the recommended ratio of 100:44 by weight.

The wood/glass/epoxy samples were made of two pieces of timber connected with butt ends with a 200 mm length of glass fibre/epoxy on each side (figure 2), and were tested with the load applied axially to the timber direction. The glass was only applied to the 100mm wide faces of the samples. The area of the joint was coated with wet resin, the glass was then positioned and resin stippled into it with a brush and then the completed joint was consolidated with a roller to expel any possible remaining air.

The joints were designed for failure by delamination of the composite by restricting their length. Tensile failure of the composite was not intended as the strength of the bond between the composite and the wood was the interesting part to test in fatigue.

At both ends of the assembled samples two shear-plate connectors were held between two steel plates and connected with a 20 mm diameter bolt in order to apply the loads (figure 3). This system was used in previous testing programmes for timber joints (11, 12, 13)

PVC and steel brackets were glued onto the timber in order to hold the LVDTs in position. The LVDTs measured displacements at the gap position between the brackets located on either piece of timber. They were fixed in a symmetrical arrangement to check any misalignment of the sample. Strain gauges were used only to measure strains in the glass fibre/epoxy layer. They were embedded directly at the surface of the composite matrix in the epoxy, with a thin coat added on top of it, while the samples were fabricated. Strain gauges were positioned in a same arrangement on each side of the sample. LVDT and strain gauges locations on the sample are shown in figures 4 and 5.

Not all the samples had the same number of strain gauges. Half of them had 6 strain gauges (3 on each side, as shown in figure 4) and the other half had only two strain gauges, one on each side, located across the gap.

13 samples were tested at different cyclic loading ranges in order to draw the S-N curve. In addition to these samples a number were tested in static loading to failure. The static results are in table 1. The cyclic loading ranges presented in table 2 are based on a proportion of the estimated failure load and were used for the tests.

Material testing

The timber planks selected for the sample fabrication were tested in three point bending before being sawn in two timber pieces. The tests were carried out at very low load to avoid any structural damage of the timber. The mid-span deflection was recorded under load. This test enabled the calculation of the apparent bending modulus of elasticity for each sample. This test was carried out to check the timber grading. Each wood/glass/epoxy sample was weighed before and after the gluing of the glass fibre/epoxy composite. This measurement enabled the calculation of the Fibre Volume Fraction (FVF), the ratio that defines the amount of glass fibre per unit weight of resin. After each test, a sample of timber was sawn from the wood/glass/epoxy joint. This sample of timber was used to measure the moisture content and the density of the joint. All these properties are presented and summarised in table 3.

Load Measurements

For the 13 samples tested, the numbers of cycles to failure were recorded for each sample and those results are presented in table 4 with indication of maximum and minimum cyclic loads.

For the samples 1 to 11, the joint failure occurred after the specified number of cycles. All samples displayed the same mode of failure: The delamination of the glass fibre/epoxy composite on both sides of the joint. However samples 12 and 13 were tested up to the number of cycles indicated on table 4 without showing any visible sign of fatigue. Considering the large number of cycles those two samples endured, the fatigue tests were stopped.

The results presented in table 4 are plotted in the S-N curve with linear maximum load versus logarithmic scale of the number of cycles, as shown in figure 6. The graph clearly indicates the linear relationship between the results of maximum load versus the logarithmic of the number of cycles.

Samples 12 and 13 were carefully removed from the testing rig following the fatigue tests. Visual inspection was carried out without revealing any visible sign of defects or cracks in the joint composite layers. Defects or cracks not visible to the naked eye could not be identified therefore it was inappropriate to state that those samples did not experience any damages from the fatigue tests. In order to estimate whether the samples were mechanically affected by the fatigue test, they were tested in static axial tension.

With a loading rate of 6kN/min, the samples were tested in tension to failure. The failure load and the modes of failure are presented in table 5.

The failure loads are below the results obtained from the joints tested in tension statically but relatively high, considering that the samples were previously tested in fatigue (the average failure load of the static tests was 34.9 kN). This indicates that sample 12 and 13 have not lost any of their tensile strength during the fatigue tests. Microscopic damage may have developed in the joints, but they were not significant enough to affect the strength of the two samples. Because they did not fail after a very large number of cycles and because after that their tensile strength was not significantly affected, it can be assumed that sample 12 and 13 were tested in tension-tension fatigue towards their endurance limits (and maybe beyond).

Strain measurements

Results were obtained from gap strain gauges (i.e. strain gauges positioned in the centre on the gap zone) and from LVDTs. Readings from the middle and end strain gauges were more scattered for most samples and therefore gave less precise results.
Fatigue strains and displacements generally increase with the number of cycles. Figure 7 shows gap strains versus cycles recorded at maximum cyclic loads for several typical joints.

The displacements from LVDTs were also recorded in the gap zone. Figure 8 shows gap displacements versus cycles recorded at maximum and minimum cyclic loads of two joints. With a 25mm original measured length a displacement of 0.1mm on this graph corresponds to a strain of 4000 microstrain.

From figure 8, it appears that the maximum gap displacements change much more significantly than the minimum gap displacements. The minimum gap displacements at low cycles even reduce up to 10000 cycles, and then rise up to the failure. The maximum gap displacements rise progressively up to approximately 10000 cycles and then rise rapidly towards failure. This effect was observed by Hacker and Ansell (3) who proposed that the first steps of strain increment correspond to the initiation and growth of fatigue cracks, as each crack initiation causes a small step in strain. Those cracks probably occur in the composite itself and at the interface between the timber and the glass fibre/epoxy.

Some joints were equipped on both faces with strain gauges in the middle and end of the glass fibre. Some of the results obtained are shown in figure 9. Because of the locations on the glass fibre, the results of middle and end strains are always lower than those obtained from the gap strains. Figure 10 shows that for a sample that was tested at slightly lower cyclic loads, such as sample 11A the strain distributions are radically different.

At lower cyclic loads, the middle and end strains behave in a different manner across the sample's fatigue life. Maximum and minimum values display the same curve shape. All values of strains remain very steady up to around 10000 cycles. Then the behaviour becomes more chaotic but still relatively constant up to the failure. It is interesting to notice that the strain distributions have the same shape and amplitude in the middle gauges as in the end gauges. Near failure, each strain has hardly increased. This clearly demonstrates that at lower cyclic loads there is less plastic strain developing. In fact middle and end strains are less affected by the cyclic loads. In theory, at some sufficiently low cyclic load, the strain distribution all over the composite surface will remain constant during the fatigue: This low load will correspond to the endurance limit of the joint.

Microscope examination

The failure mechanism that was observed for all the wood/glass/epoxy joints that failed during the fatigue tests was the delamination of the glass fibre/epoxy composite layer on both faces of the samples. Some of those composite layers were collected after the tests

and were examined using a microscope. The microscope used could take black and white pictures (100 × 80 mm) with a maximum magnifying scale of × 250.

The pictures that are presented from figure 11 to 16 were taken from composite layers, in the gap zone. All the visible fatigue damage that could be observed after the tests was in the gap of the glass fibre/epoxy composite layers. In these pictures, it appears that the matrix that once was bonded to the fibres is not there anymore. In figure 11, the matrix is visible at the top with some voids but below the fibres are not covered. The dark strip that separates the two zones is the fracture boundary, probably where the principal crack initiated in the matrix. In figure 12, the situation is rather different: the matrix is visible at the bottom (without showing any substantial voids) and the fibres are not covered at the top. The fracture boundary is clearly visible and is less regular than in figure 11. There are only six fibres that were debonded from the matrix. The presence of large voids in the matrix indicates substantial defect where cracks could initiate more easily.

Other pictures were taken in zones where fibres were debonded, as shown in figures 13 and 14. In figure 13, the matrix that is in the background, behind the fibres has an irregular surface. This confirms that some matrix cracking occurred and that the surface matrix/fibre debonding was combined with the shear failure of the matrix. Figure 14 confirms the shear failure of the matrix and the matrix/fibre debonding, as some fragments of matrix still remain bonded to the fibres.

The pictures shown in figures 15 and 16 were taken in zones with broken fibres. Figure 15 shows a broken fibre in a local matrix debonding, which is a common fatigue failure mechanism in composites. This mode of failure was observed across the fatigue tests but was very minor because the main mode of failure of the joints was not fibre breaking but composite delamination. Figure 16 shows several broken fragments of fibres orientated in various directions in a debonded matrix with many voids.

Fibre breaking seems to be a local mode of failure that probably occurred in locations where the fibre/matrix bond was poor due to the presence of voids. However the microscopic observations confirm that the main failure mode observed for the

wood/glass/epoxy joints was composite delamination from the timber all across the joint combined with fibre/matrix debonding in high stress regions such as the gap zone.

Discussion

The test results were compared with existing data from Sutherland (5). By correlating the results obtained for E-Glass and resin laminates in the DOE/MSU Database. Sutherland describes the S-N behaviour of composite materials at a constant R value using equation (1):

$$\frac{\sigma}{\sigma_0} = C' - \frac{1}{m}\log(N) = C' - b\log(N) \qquad (1)$$

Where σ is the stress level and σ_0 the static strength of the composite. *C'* is the material constant, *N* is the number of cycles and *m*, sometimes denoted *b*, is called the fatigue exponent.

In the forms of equation (1), *C' has a value of 1* when the curve that fits to the S-N data set passes through the static strength at 10^0 cycles (i.e. at static failure in the first fatigue cycle).

Equation (1) was used to characterise the DOE/MSU database. This formulation has led to the "ten percent" rule that is typically used as a general rule-of-thumb for the tensile fatigue behaviour ($R \approx 0.1$) of unidirectional composites. The fatigue strength of the composite is reduced by ten percent by each decade of fatigue cycles, when C is one and b is equal to 0.1 (i.e. the fatigue exponent m is equal to 10). This form is typically used for composites when comparing different material systems because it normalises out variations in the static strength. A large number of data points from the DOE/MSU database are plotted in figure 17.

These data are for glass fibre composites with at least 25% fibre content in the loading direction tested at R = 0.1. When applying equation (1), the good materials have a slope b of 0.10 and the poor have a slope b of 0.14. The good materials in this figure are approaching the best fatigue behaviour that can be obtained for glass fibre laminates in tensile fatigue. The small apparent variation in the fatigue slope b produces significant differences in high endurance fatigue performance. As shown in figure 17, at 20% of static strength, the good materials have almost 2.5 orders of magnitude longer life than the poor materials.

Figure 6 shows that the "ten percent" rule applies well to the data reported here. The trend line equation shown in figure 6 fits very well the previously presented equation (1) that characterised the S-N behaviour of composite materials. In fact, the material constant C' is equal to 0.94, which is very close to one. The slope of the curve b is equal to 0.1002 that corresponds to the optimum slope, according to conclusions from the DOE/MSU Database: A slope b equal to 0.10 defines the good materials as the curve is approaching the best fatigue behaviour that can be obtained for glass fibre laminates in tensile fatigue (see figure 17).

The fatigue performance may also be compared with the criteria in the design codes. Figure 18 shows the requirements of EN1995-1-1:2004 (14) from which it may be seen that $k_{fat\infty}$ is 0.15 for nailed joints and 0.25 for dowels. Comparing this with figure 6 it may be seen that there were no failures below 0.4 so a value of $k_{fat\infty}$ above 0.3 is clearly indicated for the glass/epoxy joints which is above that for dowels and nails.

Conclusions

1. Glass/epoxy joints on timber perform well in fatigue and fail in a predictable manner that is well described by conventional theories.
2. Wood/glass/epoxy joints were found to have a good fatigue resistance compared to other timber joints, according to the EN1995-1-1:2004 recommendations.

Acknowledgements.

We would like to acknowledge the support of SP systems for the supply of materials throughout this and other projects.

References

1. Benham P.P., Crawford R.J. and Armstrong C.G. 1996. *Mechanics of engineering materials*. Second Edition, Longman Group, Harlow, U.K., 1996.
2. Timber Engineering STEP1 1995 *Basis of design, materials properties, structural components and joints*. First Edition, Centrum Hout, The Netherlands, 1995
3. Hacker, C.L. and Ansell, M.P. 2001. *Fatigue damage and hysteresis in wood-epoxy laminates*. J. Mat. Sci., 36, 609-621, 2001.

4. Spera, D.A.; Esgar, J.B.; Gougeon, M. and Zuteck, M.D. 1990. *Structural properties of laminated Douglas fir/epoxy composite material*. DOE/NASA Reference Publication 1236, DOE/NASA/20320-76, Cleveland, 1990.

5. Sutherland, H.J. 1999. *On the fatigue analysis of wind turbines*. SAND99-0089, Sandia National Laboratories, Albuquerque, New Mexico, 1999.

6. Bainbridge, R. J.; Harvey, K.; Mettem, C. J.; Ansell, M. P. Fatigue Performance of Bonded-In Rods in Glulam, Using Three Adhesive Types /
meeting- International Council for Research and Innovtion in Building and Construction working commission w18 timber structures - 2000 ; 33RD ; Pages: 33-7-12

7. Masse B, Analysis of structural timber joints made with glass fibre/epoxy, PhD Thesis, Coventry University UK, 2003.

8. CP3: Chapter V: Part 2: 1972. *Code of basic data for the design of buildings: Wind loads*. British Standards Institution, London, 1972.

9. BS 5268: Part 2: 1996. *Structural use of timber. Part 2. Code of practice for permissible stress design, materials and workmanship*. British Standards Institution, London, 1996.

10. Technical Literature, SP Systems PLC, Cowes, Isle of Wight, UK.

11. P A Claisse and T Davis, High Performance Jointing Systems for Timber, Construction and Building Materials. 12(1998) 415-425

12. Davis T J and Claisse P A, Bolted Joints in Glulam and Structural Timber Composites, Construction and Building Materials, 14 (2000) 407-417

13. Davis T J and Claisse P A, Resin-injected dowel joints in glulam and structural timber composites, Construction and Building Materials, 15(2001) pp.157-167.

14. EN1995-1-1:2004 Eurocode 5. Design of timber structures. Part 1-1 General. Common rules and rules for buildings. British Standards Institution, London

Titles for Figures

Figure 1 Set of σ-log N curves for tension-tension (R = 0.1, 0.3 and 0.5) and tension-compression (R = -0.5 and -1) cyclic stress configurations). (from reference 2)

Figure 2. Detail of composite joint

Figure 3. Elevations and section of end fixing of sample to test machine

Figure 4 LVDTs and strain gauges positions on fatigue test samples.

Figure 5 Sample in position ready for the fatigue test.

Figure 6 S-N normalised curves

Figure 7 Maximum gap strain recorded for maximum cyclic loads

Figure 8 Maximum and minimum gap displacements recorded at maximum and minimum cyclic loads of 17.5 kN and 1.5 kN for two joints

Figure 9 Maximum and minimum middle and end strains recorded at maximum and minimum cyclic loads of 18.5 kN and 1.6 kN for sample 4B

Figure 10 Maximum and minimum middle and end strains recorded at maximum and minimum cyclic loads of 16 kN and 1.4 kN for sample 11A

Figures 11 and 12 Matrix/fibre debonding details at the interface with the timber (underside of the composite layer) in the gap zone.

Figures 13 and 14 Matrix/fibre cracking and shear details at the interface with the timber (underside of the composite layer) in the gap zone.

Figures 15 and 16 Fibre breaking and local debonding details at the interface with the timber in the gap zone.

Figure 17 Extremes of normalised S-N tensile fatigue data from glass fibre laminate at R = 0.1 (from reference 5).

Figure 18 Relationship between k_{fat} and the number of cycles N and the corresponding values of $k_{fat,\infty}$ as presented in EN1005-1-1:2004 (14).

Sample	**1**	**2**	**3**	**4**	**5**	**6**	**7**	**8**	**Average Values**	**Standard Deviation**
Failure Load (kN)	**32.4**	**36**	**34.8**	**35.7**	**36.6**	**36.6**	**34.2**	**33**	**34.9**	1.6
Elastic Zone (%) of failure load	76	77	86	91	89	72	96	80	83.4	8.4
Stiffness (kN/mm)	**83**	**103**	**84**	**84**	**82**	**78**	**61**	**66**	**80.1**	12.7
Elastic Deformation (mm)	0.29	0.27	0.36	0.39	0.44	0.34	0.54	0.40	0.38	0.09
Bending apparent MOE (kN/mm^2)	8.63	8.42	8.52	7.04	8.46	7.21	6.44	7.88	7.83	0.83
Moisture Content (%)	13.7	11.4	10	10.9	12.9	12.2	11.1	10.7	11.6	1.2
Fibre Volume Fraction	0.31	0.25	0.27	0.26	0.27	0.25	0.27	0.28	0.27	0.02
Density (kg/m^3)	478	516	496	517	464	495	413	454	479	35

Table 1. Results from static loading tests.

Sample	Cut from plank	Percentage of estimated load (%)	Max cyclic load (kN)	Min cyclic load (kN)
1	**D**	83	29	2.45
2	**E**	65	22.5	1.9
3	**C**	65	22.5	1.9
4	**B**	53	18.5	1.6
5	**D**	53	18.5	1.6
6	**E**	53	18.5	1.6
7	**A**	50	17.5	1.5
8	**D**	50	17.5	1.5
9	**A**	46	16	1.4
10	**C**	46	16	1.4
11	**A**	46	16	1.4
12	**B**	39	13.5	1.25
13	**C**	33	11.5	1.05

Table 2 Cyclic loading ranges for the fatigue tests.

Sample	Cut from plank	Apparent Bending MOE (kN/mm^2)	Moisture Content (%)	Fibre Volume Fraction	Density. (kg/m^3)
1	**D**	6.0	9.9	0.30	472
2	**E**	5.4	10.0	0.28	454
3	**C**	6.2	9.7	0.28	463
4	**B**	5.4	9.7	0.31	405
5	**D**	6.1	9.7	0.26	546
6	**E**	6.1	9.8	0.30	468
7	**A**	7.2	9.6	0.32	631
8	**D**	6.1	9.3	0.31	436
9	**A**	6.7	9.6	0.29	683
10	**C**	6.4	9.8	0.29	510
11	**A**	6.5	9.8	0.29	629
12	**B**	5.7	9.5	0.27	418
13	**C**	5.6	9.9	0.28	473
Average value		**6.10**	**9.72**	**0.29**	**506.8**
Standard Deviation		**0.51**	**0.20**	**0.02**	**88.7**

Table 3 Preliminary results .

Sample	Cut from plank	Max cyclic load (kN)	Min cyclic load (kN)	Cycles to failure
1	**D**	29	2.45	20
2	**E**	22.5	1.9	489
3	**C**	22.5	1.9	1391
4	**B**	18.5	1.6	2128
5	**D**	18.5	1.6	5454
6	**E**	18.5	1.6	30534
7	**A**	17.5	1.5	38400
8	**D**	17.5	1.5	54900
9	**A**	16	1.45	92330
10	**C**	15	1.4	98460
11	**A**	15	1.4	188500
12	**B**	13.5	1.25	> 186500
13	**C**	11.5	1.05	> 436250

Table 4 Tests results of loading ranges and cycles to failure.

Samples	*Cut from plank*	Failure Load (kN)	Modes of failure
12	**B**	34.8	Composite delamination on both sides
13	**C**	33.7	Composite delamination on both sides

Table 5 Results of the static tension test for sample 12 and 13.

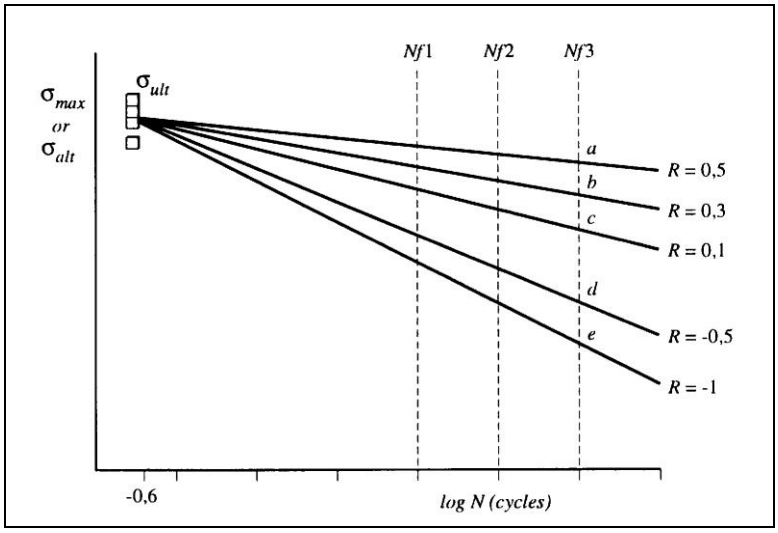

Figure 1 Set of σ-log N curves for tension-tension (R = 0.1, 0.3 and 0.5) and tension-compression (R = -0.5 and -1) cyclic stress configurations). (from reference 2)

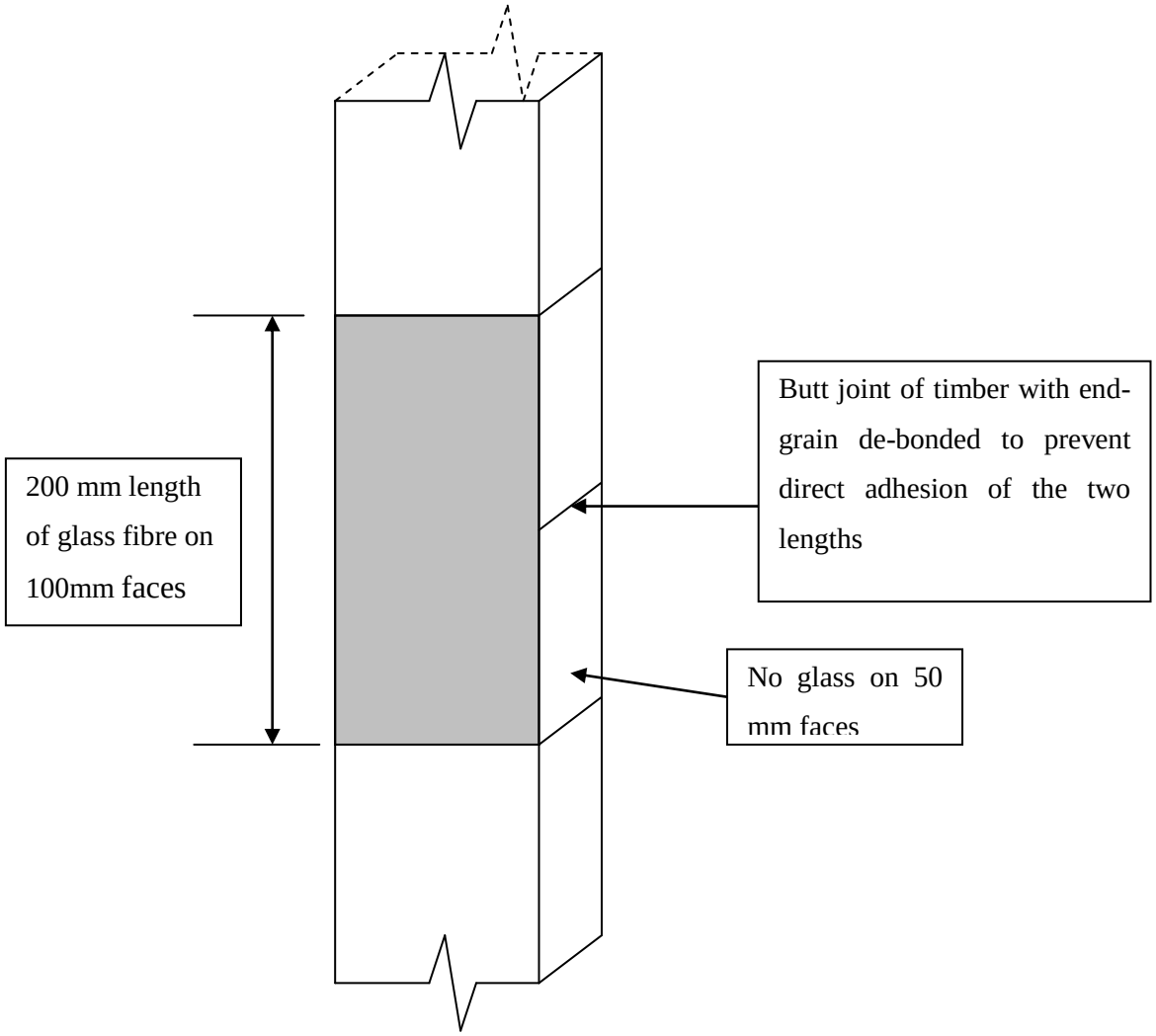

Figure 2. Detail of composite joint

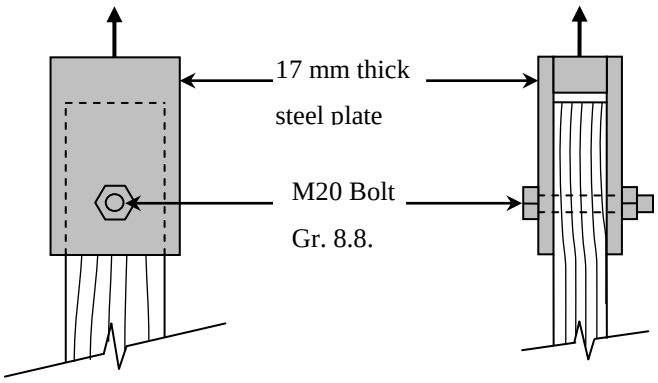

Elevations

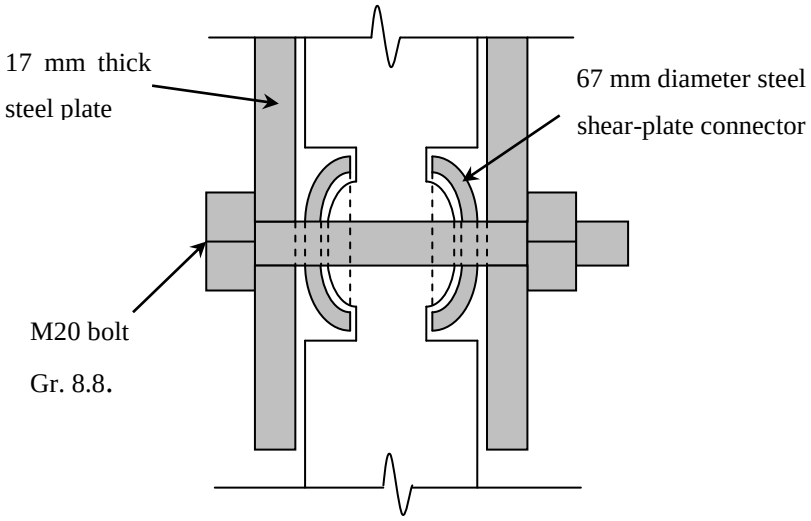

Section

Figure 3. Elevations and section of end fixing of sample to test machine

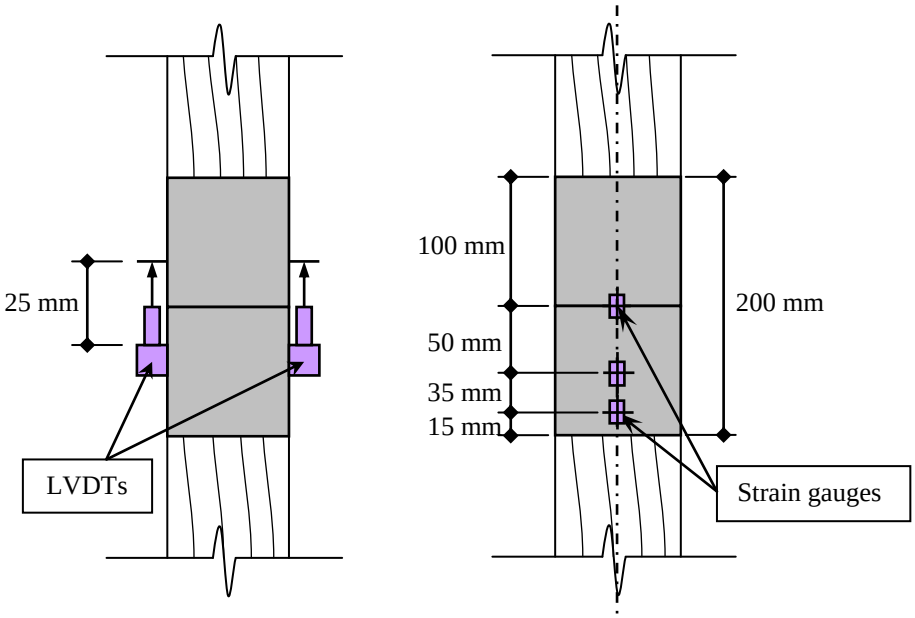

Figure 4 LVDT and strain gauge positions on fatigue test samples.

Figure 5 Sample in position ready for the fatigue test.

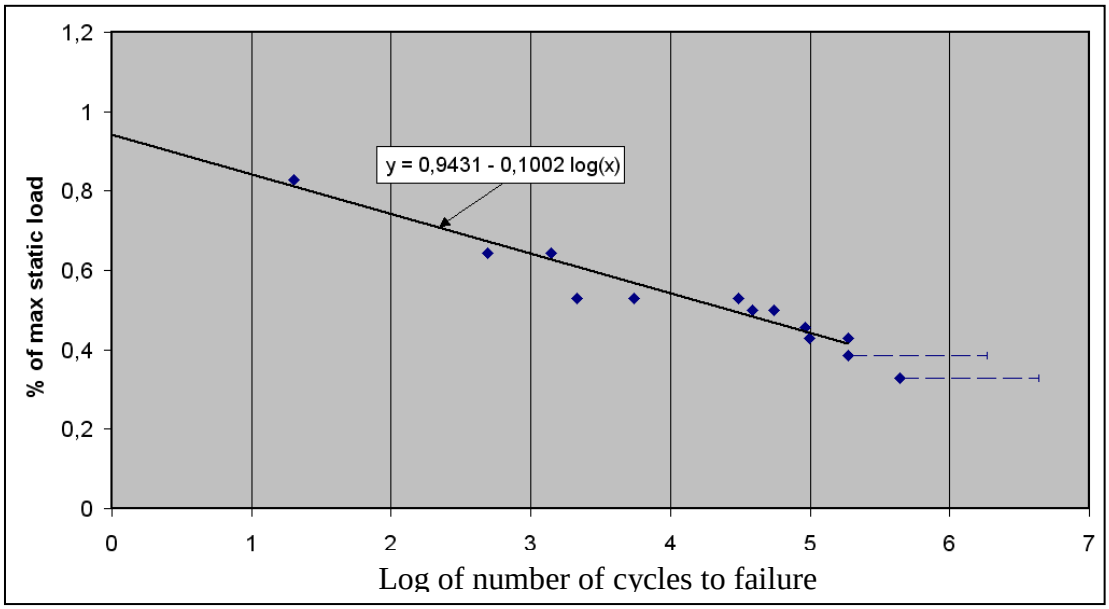

Figure 6 S-N normalised curves

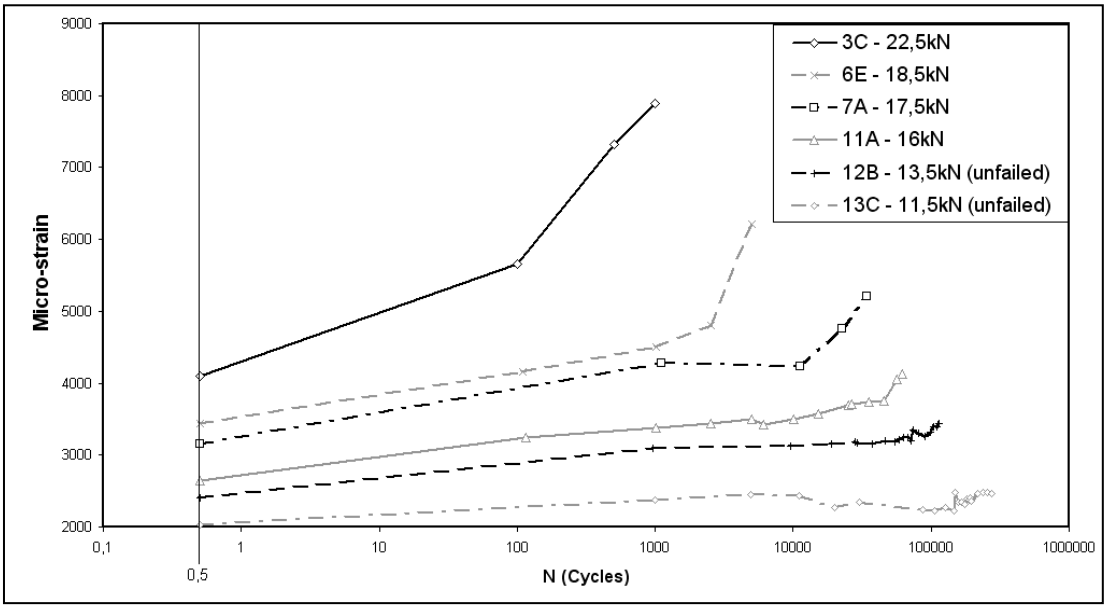

Figure 7 Maximum gap strain recorded for maximum cyclic loads

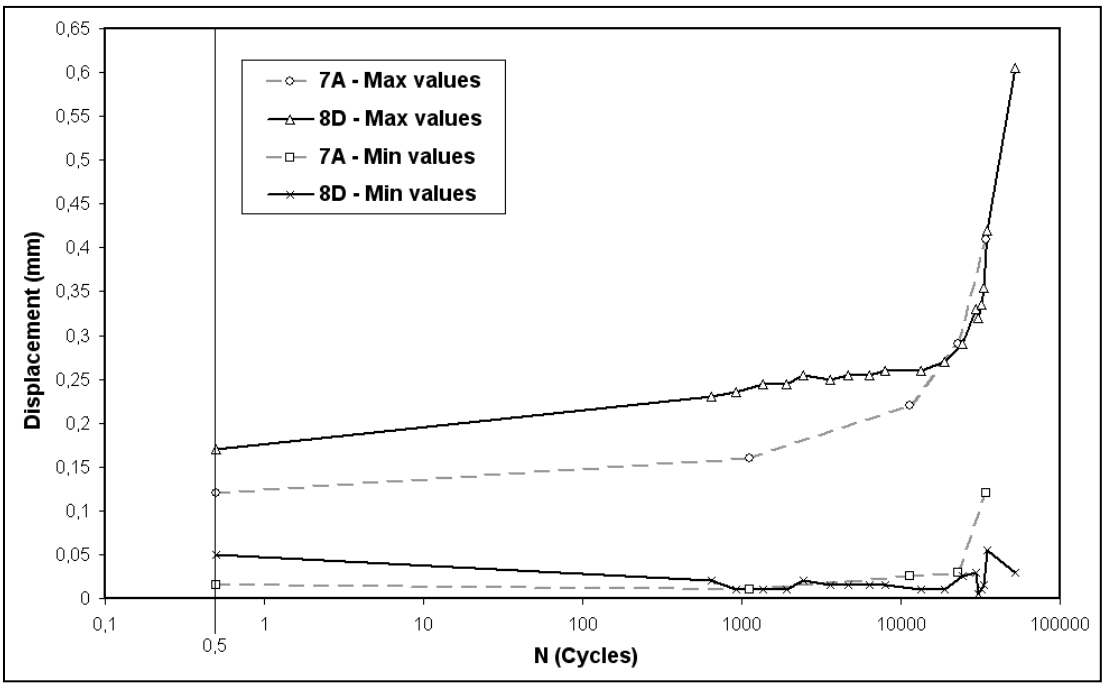

Figure 8 Maximum and minimum gap displacements recorded at maximum and minimum cyclic loads of 17.5 kN and 1.5 kN for two joints

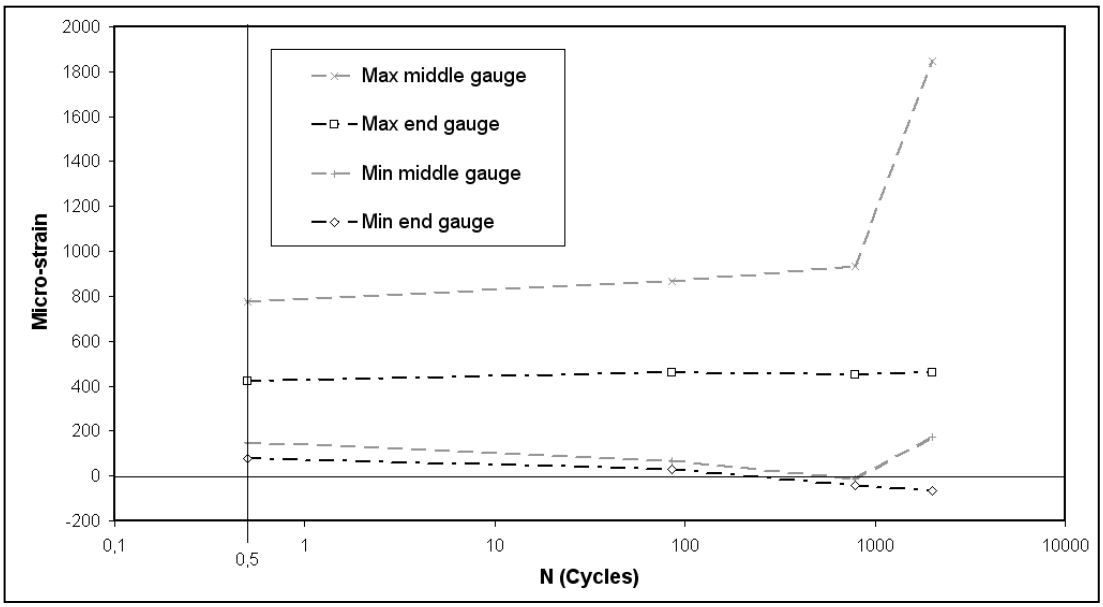

Figure 9 Maximum and minimum middle and end strains recorded at maximum and minimum cyclic loads of 18.5 kN and 1.6 kN for sample 4B

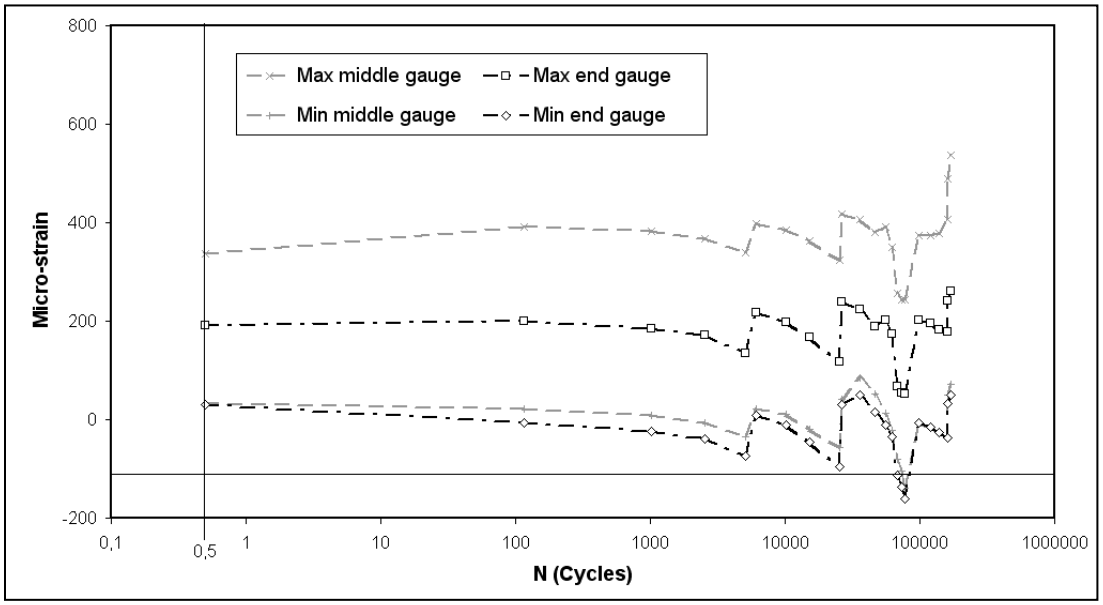

Figure 10 Maximum and minimum middle and end strains recorded at maximum and minimum cyclic loads of 16 kN and 1.4 kN for sample 11A

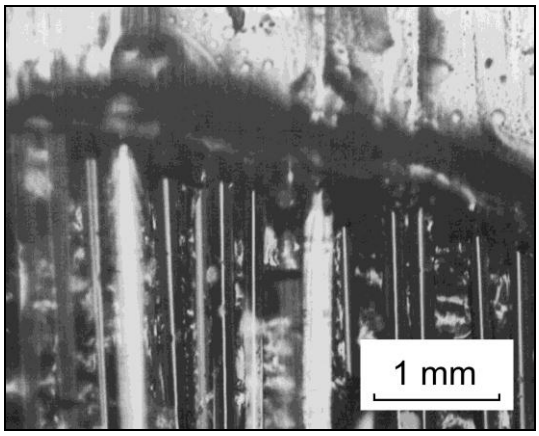

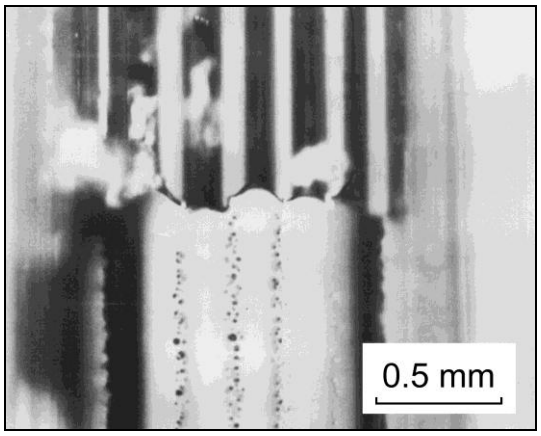

Figures 11 and 12 Matrix/fibre debonding details at the interface with the timber (underside of the composite layer) in the gap zone.

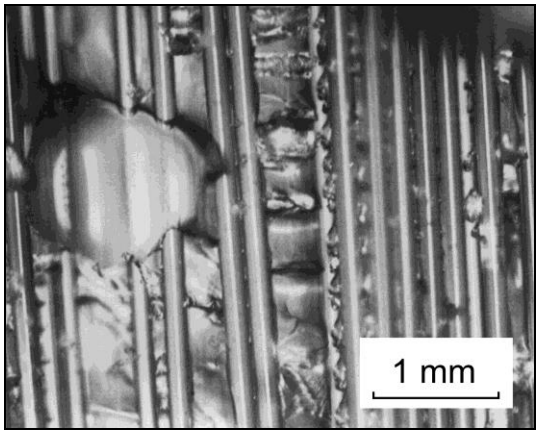

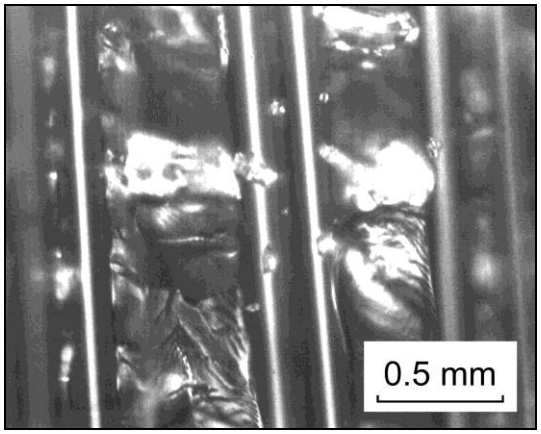

Figures 13 and 14 Matrix/fibre cracking and shear details at the interface with the timber (underside of the composite layer) in the gap zone.

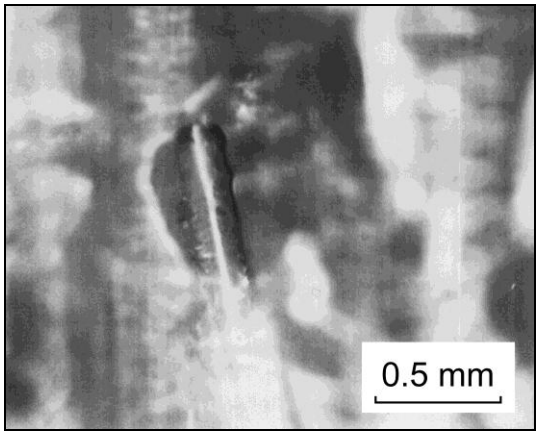

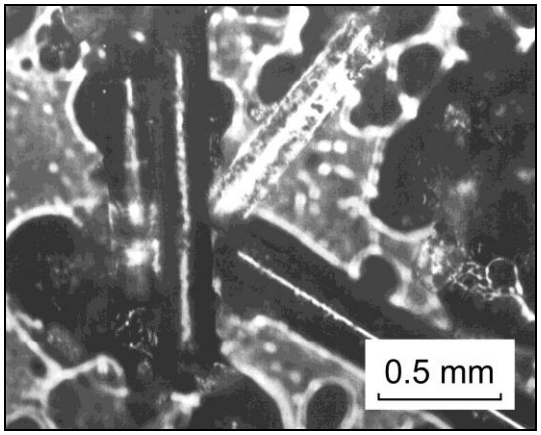

Figures 15 and 16 Fibre breaking and local debonding details at the interface with the timber in the gap zone.

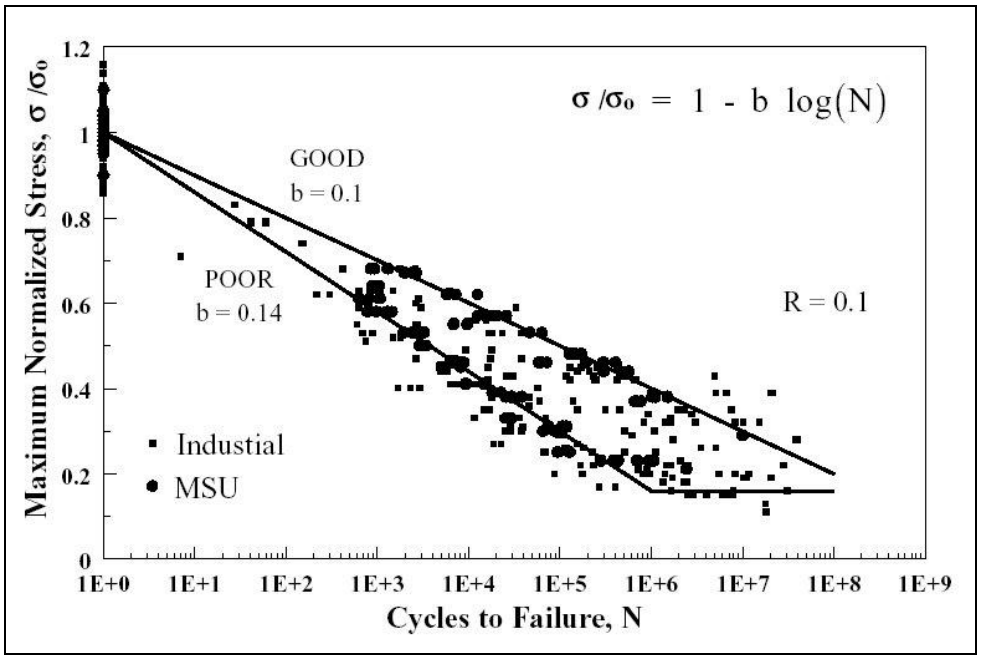

Figure 17 Extremes of normalised S-N tensile fatigue data from glass fibre laminate at R = 0.1 (from reference 5).

k_{fat}-Log N relationship	**Structural element**	$k_{fat,\infty}$
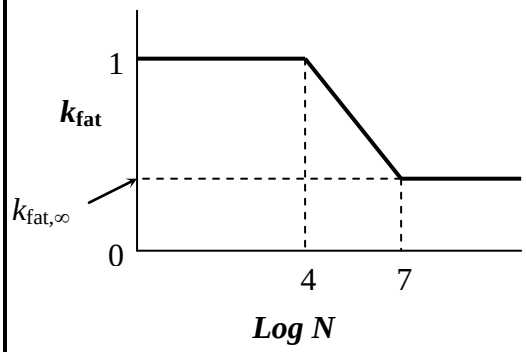	Wooden members in • Compression perpendicular and parallel to the grain • Bending, tension and reversed tension/compression • Shear Joints with • Dowels • Nails	 [0,60] [0,30] [0,20] [0,25] [0,15]

Figure 18 Relationship between k_{fat} and the number of cycles N and the corresponding values of $k_{fat,\infty}$ as presented in EN1995-1-1:2004 (14).